

Experimental realization of polarization qutrits from nonmaximally entangled states

Giuseppe Vallone,^{*} Enrico Pomarico,^{*} Francesco De Martini,^{*} and Paolo Mataloni^{*}

Dipartimento di Fisica dell'Università "La Sapienza" and Consorzio Nazionale Interuniversitario per le Scienze Fisiche della Materia, Roma, 00185 Italy

Marco Barbieri

*Dipartimento di Fisica dell'Università "La Sapienza," Roma, 00185 Italy
and Centre for Quantum Computer Technology, Department of Physics, University of Queensland, Brisbane, Queensland 4072, Australia*

(Received 16 March 2007; revised manuscript received 14 May 2007; published 18 July 2007)

Based on a recent proposal [Phys. Rev. A **71**, 062337 (2005)], we have experimentally realized two-photon polarization qutrits by using nonmaximally entangled states and linear optical transformations. By this technique, high-fidelity mutually unbiased qutrits are generated at a high brilliance level.

DOI: [10.1103/PhysRevA.76.012319](https://doi.org/10.1103/PhysRevA.76.012319)

PACS number(s): 03.67.Dd, 03.67.Hk, 03.65.Wj

I. INTRODUCTION

Shannon elected the bit as the fundamental unit of information. A system that can be only “on” or “off” is the simplest choice, but no fundamental reason prevents the adoption of $d > 2$ logical levels for information processing. Nowadays, qudits, i.e., d -level quantum systems, can be easily engineered, controlled, and measured, thus ensuring more freedom in choosing which dimensionality to use. The interest in these systems resides in the fact that dealing with arbitrary dimensions may allow one to simplify the general structure of a quantum protocol. Moreover, quantum key distribution schemes have been demonstrated to be more resilient to a specific class of eavesdropping attacks when qutrits ($d=3$) or ququads ($d=4$) are adopted instead of qubits [1–4]. Multilevel systems and, in particular, qutrits are shown to be more efficient also for designing other security protocols, e.g., bit commitment or coin tossing [5,6], and for fundamental tests of quantum mechanics [7–9].

Some optical realizations and applications of qutrits, exploiting different physical processes, have been demonstrated [10]. Time-bin entangled qudits are generated by a time-frequency entangled photon pair through a multiarmed Franson interferometer [7]. In this case, the dimensionality d is given by the number of arms. This scheme presents a certain rigidity in switching among different states. A different approach exploits orbital angular momentum entanglement of single photons generated by spontaneous parametric down-conversion (SPDC), but only partial control of the qutrit state is provided. Indeed, in the method of Refs. [5,10–12] a specific hologram is needed for each qutrit state. Transverse momentum correlation has also been used to realize spatial bins [13,14]. However, in this case also it seems unclear how to perform the rotation of the generated state efficiently.

More recently, the experimental realization of arbitrary qutrit states, adopting the polarization degree of freedom of a two-photon state, was reported [15]. By this technique, three parametric sources, two type-I and one type-II nonlinear

crystals, placed, respectively, within and outside an interferometer, are illuminated by a common laser, and determine the critical adjustment of the qutrit phase. Moreover, the two collinear photons determining the qutrit state are divided by a symmetric beam splitter. This contributes to further reduction of the quite low production rate of the three-level systems.

It is worth noting that qutrits have also been prepared by postselection from a four-photon entangled state [16].

In this paper, we present the experimental realization of the proposal of Ref. [17] to generate qutrits by using a single nonlinear crystal and linear optical elements such as wave plates. Qutrits are encoded in the polarization of two photons initially prepared in a nonmaximally entangled state, which plays the role of a “seed” state. Mutually unbiased bases can be obtained by linear optical transformations acting on two different seeds. This technique presents the advantage of merging accurate control and flexibility in the generation of the state at a high brilliance level.

The paper is organized as follows. Section II concerns the description of the theoretical proposal of [17]. We explain how to generate a two-photon polarization qutrit starting from a nonmaximally entangled state and using linear optics elements. Section III shows the experimental results obtained by our technique. First, we describe the source of entangled photons used in our experiment (Sec. III A) and present the experimental realization of the seed states (Sec. III B). Then, in Secs. III C and III D, the last stage of qutrit preparation, namely, the application of unitary transformations to each photon, is shown.

II. THEORY

Let us consider the polarization qutrit

$$|\xi_{\psi,\phi}\rangle = \frac{1}{\sqrt{3}}(|H\rangle_1|H\rangle_2 + e^{i\psi}|V\rangle_1|V\rangle_2 + e^{i\phi}|\psi^+\rangle_{12}), \quad (1)$$

where 1 and 2 label the two particles, $|H\rangle$ and $|V\rangle$ correspond to the horizontal and vertical polarization states, and $|\psi^+\rangle_{12} = (1/\sqrt{2})(|H\rangle_1|V\rangle_2 + |V\rangle_1|H\rangle_2)$ is one of the four polarization Bell states. The states in Eq. (1) span the symmetrical subspace of the two-qubit Hilbert space.

^{*}<http://quantumoptics.phys.uniroma1.it/>

We are interested in the generation of a set of mutually unbiased (MU) bases, which are the basic tool for quantum key distribution [1,18]. For this purpose, we require that, in the superposition state (1), the three terms of the computational basis $\{|H\rangle_1|H\rangle_2, |V\rangle_1|V\rangle_2, |\psi^+\rangle_{12}\}$ appear with the same probability amplitude. Indeed, our method is suitable for adjusting at the same time both the balance between the three contributions and the phases ϕ and ψ needed to obtain MU bases.

Such states are obtained by applying two unitaries to a seed nonmaximally entangled state,

$$|\chi_{\psi,\phi}\rangle = d_H|H\rangle_1|H\rangle_2 + d_V|V\rangle_1|V\rangle_2. \quad (2)$$

The dependence on the phases ψ and ϕ is implicit in d_H and d_V , which are chosen to be real numbers:

$$d_H = |x_+|, \quad d_V = |x_-|, \quad (3)$$

where

$$x_{\pm} = \frac{\sqrt{2} \pm e^{i(\phi-\psi/2)}}{\sqrt{6}}. \quad (4)$$

We can write explicitly the transformation that maps the seed state $|\chi_{\psi,\phi}\rangle$ into the desired qutrit state as

$$|\xi_{\psi,\phi}\rangle = (U \otimes W)|\chi_{\psi,\phi}\rangle, \quad (5)$$

up to an irrelevant global phase. The two unitaries U and W , applied to photons 1 and 2, respectively, and expressed in the $\{|H\rangle, |V\rangle\}$ basis, are

$$W = \underbrace{\begin{pmatrix} 1 & 0 \\ 0 & e^{i\alpha} \end{pmatrix}}_{P_\alpha} \underbrace{\frac{1}{\sqrt{2}} \begin{pmatrix} 1 & 1 \\ -1 & 1 \end{pmatrix}}_{H'}, \quad \alpha = \frac{\psi}{2} + \pi \quad (6)$$

$$U = W \begin{pmatrix} 1 & 0 \\ 0 & e^{i\Gamma} \end{pmatrix}, \quad \Gamma = \arg\left(\frac{x_-}{x_+}\right). \quad (7)$$

The phase shift Γ can be introduced contextually with the generation of the seed state. Indeed, thanks to the explicit expressions of U and W , Eq. (1) can be written as

$$|\xi_{\psi,\phi}\rangle = (P_\alpha \otimes P_\alpha)(H' \otimes H')|\chi'_{\psi,\phi}\rangle, \quad (8)$$

where

$$|\chi'_{\psi,\phi}\rangle = d_H|H\rangle_1|H\rangle_2 + e^{i\Gamma}d_V|V\rangle_1|V\rangle_2, \quad (9)$$

and the unitaries P_α and H' are defined in (6). The gate P_α represents a phase shifter that adds a phase difference $\alpha = \psi/2 + \pi$ between the states $|V\rangle$ and $|H\rangle$. The gate H' (similar to the Hadamard gate) performs the transformations $|H\rangle \rightarrow (1/\sqrt{2})(|H\rangle - |V\rangle)$ and $|V\rangle \rightarrow (1/\sqrt{2})(|H\rangle + |V\rangle)$.¹ These unitaries are attainable by simple linear optical elements such as wave plates.

As said, we are interested, in particular, in generating three sets of MU bases. The (nine) vectors corresponding to

the three basis sets, all expressed in the form of Eq. (1), are explicitly given in the following:

$$(1) \quad \left\{ \begin{array}{l} |v_1\rangle = \frac{1}{\sqrt{3}}(|HH\rangle + |VV\rangle + |\psi^+\rangle), \\ |v_2\rangle = \frac{1}{\sqrt{3}}(|HH\rangle + e^{(2/3)\pi i}|VV\rangle + e^{-(2/3)\pi i}|\psi^+\rangle), \\ |v_3\rangle = \frac{1}{\sqrt{3}}(|HH\rangle + e^{-(2/3)\pi i}|VV\rangle + e^{(2/3)\pi i}|\psi^+\rangle), \end{array} \right. \quad (10)$$

$$(2) \quad \left\{ \begin{array}{l} |w_1\rangle = \frac{1}{\sqrt{3}}(|HH\rangle + e^{-(2/3)\pi i}|VV\rangle + e^{-(2/3)\pi i}|\psi^+\rangle), \\ |w_2\rangle = \frac{1}{\sqrt{3}}(|HH\rangle + e^{(2/3)\pi i}|VV\rangle + |\psi^+\rangle), \\ |w_3\rangle = \frac{1}{\sqrt{3}}(|HH\rangle + |VV\rangle + e^{(2/3)\pi i}|\psi^+\rangle), \end{array} \right. \quad (11)$$

$$(3) \quad \left\{ \begin{array}{l} |z_1\rangle = \frac{1}{\sqrt{3}}(|HH\rangle + e^{(2/3)\pi i}|VV\rangle + e^{(2/3)\pi i}|\psi^+\rangle), \\ |z_2\rangle = \frac{1}{\sqrt{3}}(|HH\rangle + e^{-(2/3)\pi i}|VV\rangle + |\psi^+\rangle), \\ |z_3\rangle = \frac{1}{\sqrt{3}}(|HH\rangle + |VV\rangle + e^{-(2/3)\pi i}|\psi^+\rangle). \end{array} \right. \quad (12)$$

Note that, in order to obtain a full set of MU bases, a fourth one, namely, $\{|HH\rangle, |VV\rangle, |\psi^+\rangle\}$, must be considered [19].

We give in Table I the explicit values of α , d_H , d_V , and Γ for all the states in the three MU bases. Detailed calculations are given in the Appendix.

III. EXPERIMENT

In this section, we explain how to implement the procedure described in Sec. II and show the experimental results obtained. From Eqs. (8) and (9), it follows that all the states $|\xi_{\psi,\phi}\rangle$, expressed as (1), can be produced in four steps.

(I) Choose ϕ and ψ and generate the corresponding (non-maximally entangled) seed state $|\chi_{\psi,\phi}\rangle$.

(II) Change the relative phases between $|H\rangle_1|H\rangle_2$ and $|V\rangle_1|V\rangle_2$ in order to obtain $|\chi'_{\psi,\phi}\rangle$.

(III) Apply the gates H' to each photon. This is performed by a half-wave plate (HWP) whose axis is at -22.5° with respect to the horizontal direction.

(IV) Apply the phase shifter P_α to each photon. This phase shift is realized by a birefringent medium, e.g., a quarter-wave plate (QWP), with the optical axis oriented in the horizontal plane. The corresponding induced phase α is varied by rotating the plate along its vertical axis (see Fig. 1).

In the actual realization we performed step III before step II. In this way the phase Γ can be easily set by considering

¹Note that the transformation H' , is related to the usual Hadamard transformation H by a unitary matrix, i.e., $H' = \sigma_z H$, where σ_z is the usual Pauli matrix.

TABLE I. Theoretical values of α , d_H , d_V , and Γ for the states of the MU bases.

	ψ	ϕ	α	d_H	d_V	Γ
$ v_1\rangle$	0	0	0	$\frac{\sqrt{2}-1}{\sqrt{6}}$	$\frac{\sqrt{2}+1}{\sqrt{6}}$	0
$ v_2\rangle$	$\frac{2}{3}\pi$	$-\frac{2}{3}\pi$	$-\frac{2}{3}\pi$			
$ v_3\rangle$	$-\frac{2}{3}\pi$	$\frac{2}{3}\pi$	$\frac{2}{3}\pi$			
$ w_1\rangle$	$-\frac{2}{3}\pi$	$-\frac{2}{3}\pi$	$\frac{2}{3}\pi$	$\sqrt{\frac{3+\sqrt{2}}{6}}$	$\sqrt{\frac{3-\sqrt{2}}{6}}$	$\arcsin \sqrt{\frac{6}{7}}$
$ w_2\rangle$	$\frac{2}{3}\pi$	0	$-\frac{2}{3}\pi$			
$ w_3\rangle$	0	$\frac{2}{3}\pi$	0			
$ z_1\rangle$	$\frac{2}{3}\pi$	$\frac{2}{3}\pi$	$-\frac{2}{3}\pi$	$\sqrt{\frac{3+\sqrt{2}}{6}}$	$\sqrt{\frac{3-\sqrt{2}}{6}}$	$-\arcsin \sqrt{\frac{6}{7}}$
$ z_2\rangle$	$-\frac{2}{3}\pi$	0	$\frac{2}{3}\pi$			
$ z_3\rangle$	0	$-\frac{2}{3}\pi$	0			

that the $H' \otimes H'$ gate transforms the seed $|\chi'\rangle$ in the following way:

$$H' \otimes H' |\chi'\rangle = \frac{d_H + e^{i\Gamma} d_V}{2} (|HH\rangle + |VV\rangle) - \frac{d_H - e^{i\Gamma} d_V}{\sqrt{2}} |\psi^+\rangle. \quad (13)$$

For fixed values of d_H and d_V , the value of Γ determines the relative weight of $|HH\rangle$ (or $|VV\rangle$) and $|\psi^+\rangle$. In this way, the value of Γ is chosen in order to make equal the two weights.

A. Parametric source

Photon pairs are generated by a SPDC source whose detailed description is given in [20–22]. It allows the efficient generation of the polarization entangled states $|\Phi_\theta\rangle = (1/\sqrt{2})(|H\rangle_1|H\rangle_2 + e^{i\theta}|V\rangle_1|V\rangle_2)$ by using a type-I, 0.5-mm-thick, β -BaB₂O₄ (BBO) crystal. In the source, the entanglement arises from the superposition of the degenerate parametric emissions ($\lambda=728$ nm) of the crystal, excited in two opposite directions \vec{k}_p and $-\vec{k}_p$ by a V-polarized argon

laser beam ($\lambda_p=364$ nm). In the following, we will refer to the emission excited in the direction \vec{k}_p as the “left” emission (i.e., on the left of the BBO crystal in Fig. 1), while the emission excited in the direction $-\vec{k}_p$ is the “right” one. The H-polarized photons belonging to the “left” emission are transformed $|H\rangle \rightarrow |V\rangle$ by a double passage through a quarter-wave plate ($\lambda/4$ in Fig. 1). The phase θ can be easily set by a micrometric translation of the spherical mirror M . Parametric radiation is coupled to two single-mode fibers, achieving a coincidence level of ~ 1000 s⁻¹, over the 20 nm bandwidth of two interference filters (IF, Fig. 1).

Using this source, we can easily generate the states $|HH\rangle$, $|VV\rangle$, and $|\psi^+\rangle$. The first two states are simply obtained by selecting only the right or left emission, with fidelities $F_{|HH\rangle} = 0.991 \pm 0.010$ and $F_{|VV\rangle} = 0.960 \pm 0.008$. The state $|\psi^+\rangle$ can be generated from the state $|\Phi_0\rangle$ by applying a HWP at 45° on one photon, obtaining the fidelity $F_{|\psi^+\rangle} = 0.966 \pm 0.008$. The fidelities of $|HH\rangle$ and $|VV\rangle$ are different, mainly because of the nonideal behavior of the $\lambda/4$ wave plate. Indeed, the operational wavelength of all the wave plates adopted in our experiment is equal to 750 nm. As we shall see below, this feature partially affects the overall fidelities of the generated qutrits.

Another possible source of imperfection arises from the critical spatial matching between the right and left parametric emission. This is overcome by the adoption of a thin crystal and single-mode fibers. Moreover, by this scheme no temporal or spatial crystal walkoff is present with type-I phase matching.

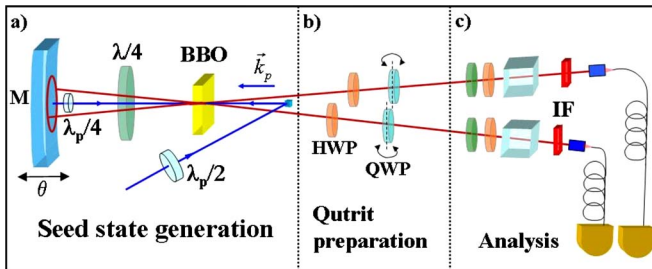


FIG. 1. (Color online) Optical setup for generation and analysis of polarization qutrits. (a) The entanglement source is used to produce the seed state. The reciprocal weights of the $|H\rangle_1|H\rangle_2$ and $|V\rangle_1|V\rangle_2$ components are set by controlling the pump beam polarization in the first passage through the β -BaB₂O₄ (BBO) by the $\lambda_p/2$ half-wave plate and in the second passage by the $\lambda_p/4$ quarter-wave plate. (b) The qutrit is encoded by applying the $H' \otimes H'$ transformation by two HWP plates and by proper phase shifts $P_\alpha \otimes P_\alpha$ performed by QWP plates. (c), Finally the state is characterized by polarization quantum state tomography.

B. Seed state generation (step I)

The generation of nonmaximally entangled states by the SPDC source described above was previously demonstrated in Ref. [23]. The basic idea consists of tuning the polarization of the pump beam so that the nonlinear gain for the SPDC process can be varied. Indeed, if the pump beam is linearly polarized at an angle Θ_p with respect to the BBO optic axis, the SPDC probability is $p \propto \cos^2 \Theta_p$. Therefore, by inserting a QWP intercepting only the pump beam between the BBO and the mirror M ($\lambda_p/4$ in Fig. 1), the right emis-

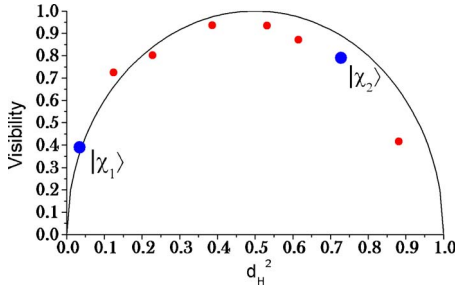


FIG. 2. (Color online) Visibility (V) of nonmaximally entangled state $|\chi\rangle$ vs the $|HH\rangle$ weight d_H^2 . The black line represents the theoretical curve $V=2\sqrt{d_H^2(1-d_H^2)}$. Error bars are smaller than the point symbols.

sion probability becomes lower, and the seed state

$$|\chi'\rangle = d_H|HH\rangle + e^{i\Gamma}d_V|VV\rangle, \quad d_H < d_V, \quad (14)$$

is generated. The phase Γ is set by finely translating the spherical mirror, as said. On the other hand, seed states with higher $|HH\rangle$ component ($d_H > d_V$) can be generated by inserting a further HWP before the BBO crystal ($\lambda_p/2$ in Fig. 1). In this way, by changing the \vec{k}_p pump polarization, we lower the efficiency for the left emission. The $\lambda_p/4$ wave plate is used to rotate back the $-\vec{k}_p$ beam polarization to the vertical direction, thus raising the right emission. Then the states

$$|\chi'\rangle = d_H|HH\rangle + e^{i\Gamma}d_V|VV\rangle, \quad d_H > d_V, \quad (15)$$

are generated.

For our experiment, two different seed states are needed (see Table I), namely,

$$|\chi_1\rangle = \frac{\sqrt{2}-1}{\sqrt{6}}|HH\rangle + \frac{\sqrt{2}+1}{\sqrt{6}}|VV\rangle \approx 0.169|HH\rangle + 0.986|VV\rangle,$$

$$|\chi_2\rangle = \sqrt{\frac{3+\sqrt{2}}{6}}|HH\rangle + \sqrt{\frac{3-\sqrt{2}}{6}}|VV\rangle \approx 0.858|HH\rangle + 0.514|VV\rangle. \quad (16)$$

The first seed state $|\chi_1\rangle$ is used for the first basis set $\{|v_a\rangle\}$, while the second seed state $|\chi_2\rangle$ is used for the remaining two sets, namely, $\{|w_a\rangle\}$ and $\{|z_a\rangle\}$. Note that the intrinsic difficulty in implementing the first state is due to the required lack of balance of the two contributions, $d_H^2/d_V^2 \approx 0.03$, almost comparable with the experimental uncertainties associated with each polarization contribution.

We show in Fig. 2 the visibility $V=(N_{max}-N_{min})/(N_{max}+N_{min})$ of different nonmaximally entangled states as a function of the probability d_H^2 of $|HH\rangle$. It is calculated by the coincidences of the two photons measured in the diagonal component $(1/\sqrt{2})(|H\rangle+|V\rangle)$ varying the phase Γ from 0 to π . N_{max} (N_{min}) are the coincidence counts corresponding to $\Gamma=0$ ($\Gamma=\pi$). The two large blue points refer to the states $|\chi_1\rangle$ and $|\chi_2\rangle$. The points on the left ($d_H^2 < 0.5$) are closer to the theoretical curve probably because only the insertion of $\lambda_p/4$ is required for those states.

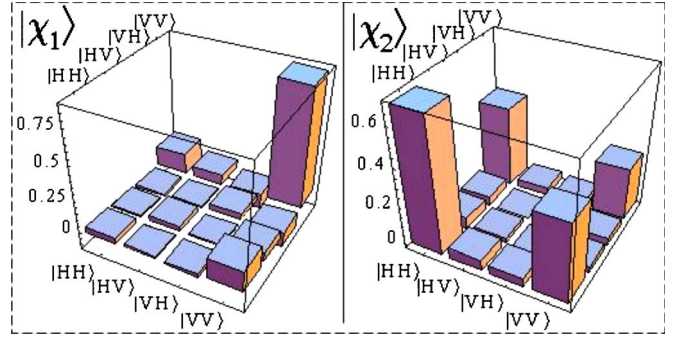


FIG. 3. (Color online) Experimental quantum tomographies (real parts) of the seed states $|\chi_1\rangle$ and $|\chi_2\rangle$ expressed in the $\{|HH\rangle, |HV\rangle, |VH\rangle, |VV\rangle\}$ basis. For the two states we obtain the purities $\mathcal{P}_{|\chi_1\rangle}=0.908\pm 0.034$ and $\mathcal{P}_{|\chi_2\rangle}=0.930\pm 0.036$. The imaginary components are negligible.

For a complete characterization of the two seed states (16), we performed a complete quantum tomography of the states; the resulting diagrams are shown in Fig. 3. We used the maximum likelihood estimation method described in [24], obtaining the fidelity $F_1=0.912\pm 0.010$ for $|\chi_1\rangle$ and $F_2=0.946\pm 0.016$ for $|\chi_2\rangle$. We also measured the trace of the square of the experimental density matrix, i.e., the purity of the generated states $\mathcal{P}_\rho=\text{Tr}(\rho^2)$. The results are given in the caption of Fig. 3.

C. H' gate and Γ phase setting (steps II and III)

The following steps for qutrit generation correspond to applying the H' transformation (Fig. 1) and the Γ phase setting to each photon. As said, the $H' \otimes H'$ transformation is performed by the action of two HWP's oriented at -22.5° with respect to the vertical direction.

The phase Γ needed for the $|\chi'\rangle$ generation is set, as already said, after the insertion of the half-wave plates that implement the unitary gate $H' \otimes H'$. The correct position is changed by micrometric translation of the mirror M (see Fig. 1) and fixed by observing that the count rate for $|H\rangle_1|H\rangle_2$ events doubles that of the $|H\rangle_1|V\rangle_2$ contribution.

It is evident from Table I that the states $|v_1\rangle$, $|w_3\rangle$, and $|z_3\rangle$ can be generated by applying only the previous operations, i.e., without the need to insert the phase gates $P_\alpha \otimes P_\alpha$. The corresponding experimental density matrices are shown in Fig. 4, with fidelities $F_{|v_1\rangle}=0.949\pm 0.010$, $F_{|w_3\rangle}=0.931\pm 0.011$, and $F_{|z_3\rangle}=0.932\pm 0.010$. Here and in the following, we will use the basis $\{|HH\rangle, |VV\rangle, |\psi^+\rangle, |\psi^-\rangle\}$, in order to have a better comparison with (1). These states are obtained by the insertion of two half-wave plates (HWP in Fig. 1) and correct phase Γ setting (see Table I), as said.

D. Phase gate (step IV)

The implementation of the last gate of the protocol, namely, the $P_\alpha \otimes P_\alpha$ operation, is realized by inserting for each photon a QWP with vertical optical axis. It is mounted on a rotating stage which allows the actual thickness to be tuned. In this way, different phase shifts between the vertical and horizontal polarization components are achieved. In Fig.

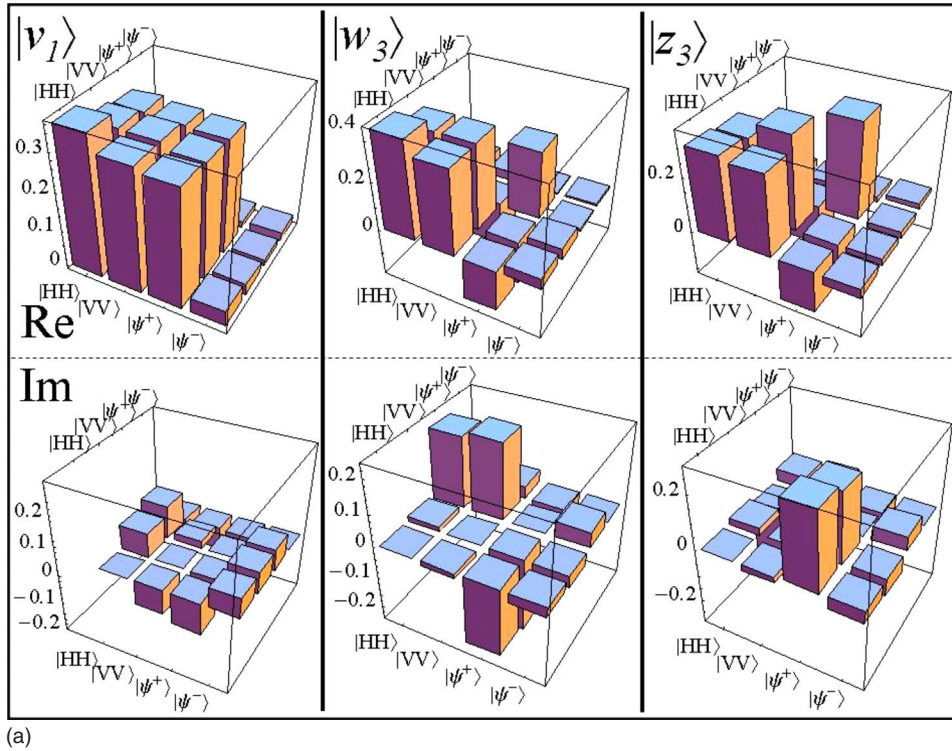
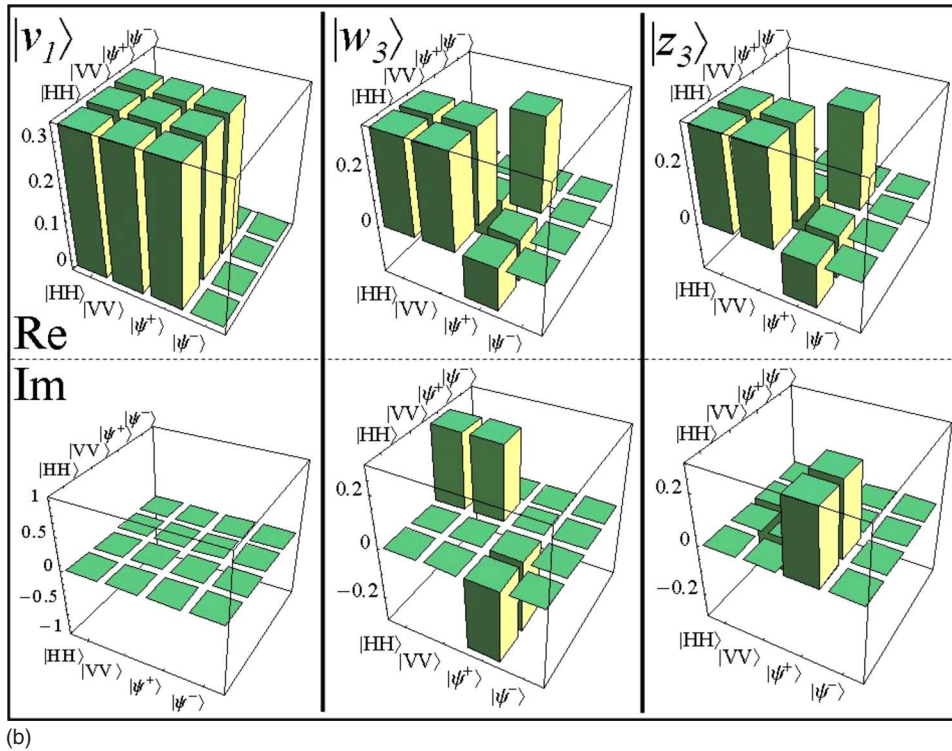


FIG. 4. (Color online) Experimental quantum tomography (a) and theoretical density matrices (b) of the states $|v_1\rangle$, $|w_3\rangle$, and $|z_3\rangle$. The upper pictures represent the real (Re) parts of the density matrices, while the lower pictures represent the imaginary (Im) parts. We measured the purities $\mathcal{P}_{|v_1\rangle}=0.974\pm 0.030$, $\mathcal{P}_{|w_3\rangle}=0.904\pm 0.033$, and $\mathcal{P}_{|z_3\rangle}=0.895\pm 0.028$.



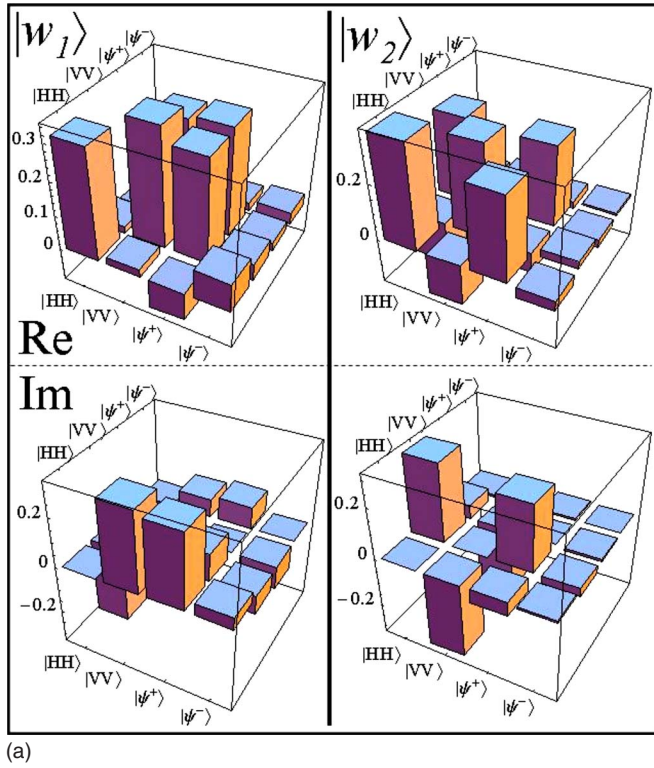
5 we show the two states $|w_1\rangle$ and $|w_2\rangle$ obtained by implementing the gate. The experimental fidelities are $F_{|w_1\rangle}=0.901\pm 0.010$ and $F_{|w_2\rangle}=0.939\pm 0.009$.

We also generated the two remaining states of the $|z_a\rangle$ basis (see Fig. 6). The experimental fidelities are given by $F_{|z_1\rangle}=0.918\pm 0.009$ and $F_{|z_2\rangle}=0.933\pm 0.009$. We did not actually generate the other two states $|v_2\rangle$ and $|v_3\rangle$ of the fourth basis, but we expect similar results for them. However, it is

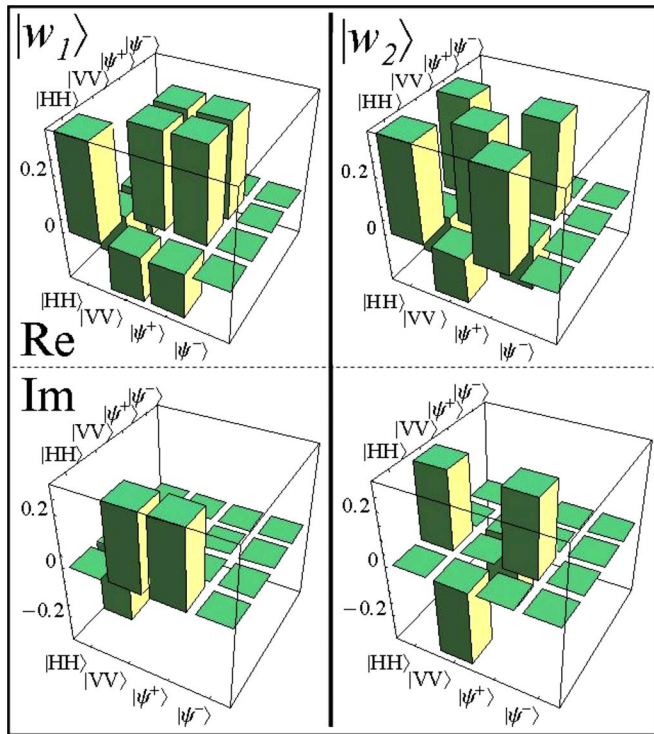
well known that a qutrit-based quantum key distribution adopting only three mutually unbiased bases is more secure than qubit-based schemes [1]. Furthermore, it allows a higher transmission rate.

IV. CONCLUSIONS

In this paper, we have shown the experimental feasibility of the proposal given in [17] for the realization of polariza-



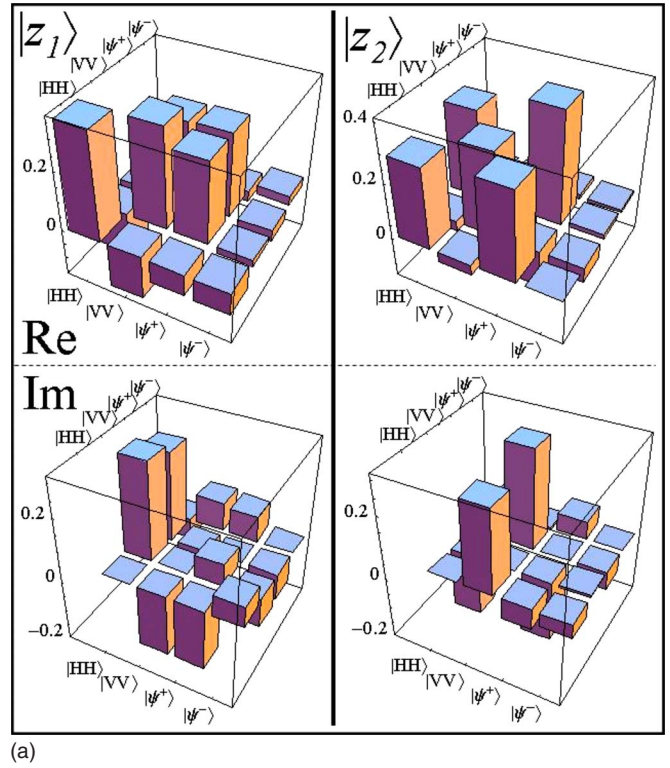
(a)



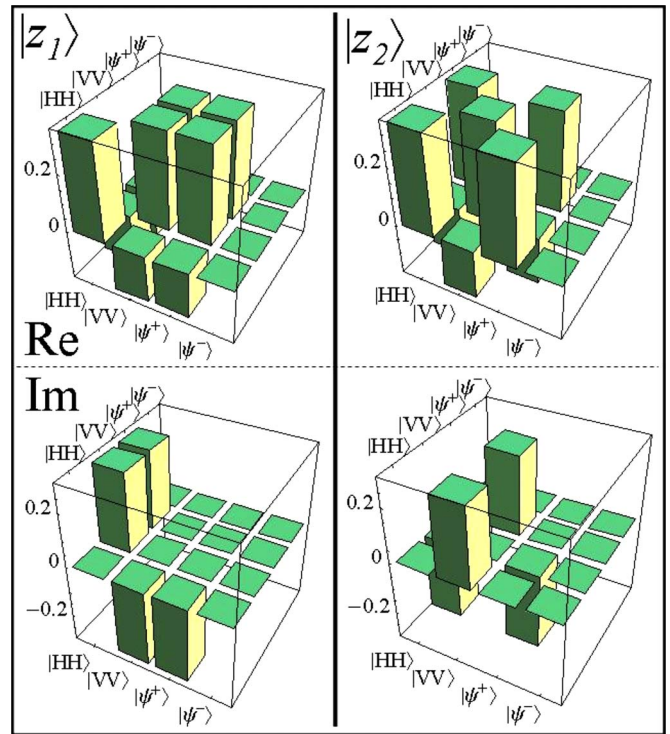
(b)

FIG. 5. (Color online) Experimental quantum tomography (a) and theoretical density matrices (b) of the states $|w_1\rangle$ and $|w_2\rangle$. We have the purities $\mathcal{P}_{|w_1\rangle}=0.969\pm 0.030$ and $\mathcal{P}_{|w_2\rangle}=0.918\pm 0.024$.

tion qutrit states. The protocol starts from the generation of a two-photon nonmaximally entangled state, and is based on the application of two unitary transformations to each photon. Each relevant parameter of the qutrit states can be easily



(a)



(b)

FIG. 6. (Color online) Experimental quantum tomography (a) and theoretical density matrices (b) of the states $|z_1\rangle$ and $|z_2\rangle$. We have the purities $\mathcal{P}_{|z_1\rangle}=0.931\pm 0.028$ and $\mathcal{P}_{|z_2\rangle}=0.937\pm 0.032$.

tuned by this protocol. The experimental procedure can be described in four steps; we showed the experimental results corresponding to each step, demonstrating in this way the actual implementation of the procedure. This method is very

powerful, as demonstrated by the high coincidence rate and the high values of fidelities of the states. Moreover, the simplicity of this scheme could allow an easy experimental implementation of quantum security protocols.

ACKNOWLEDGMENTS

We thank Massimiliano Sacchi and Mauro D'Ariano for useful discussions. This work was supported by the PRIN'05 ("New Perspectives in Entanglement and Hyperentanglement Generation and Manipulation") of MIUR (Italy).

APPENDIX: CALCULATION

In this section, we describe in detail how the transformations U and W , which generate the state (1), are found.

Note that the state $|\xi_{\phi,\psi}\rangle$ can also be written as

$$|\xi_{\phi,\psi}\rangle = (\Lambda \otimes 1)(|H\rangle_1|H\rangle_2 + |V\rangle_1|V\rangle_2), \quad (\text{A1})$$

where the matrix Λ acting on photon 1 is written in the basis $\{|H\rangle, |V\rangle\}$ as

$$\Lambda = \frac{1}{\sqrt{3}} \begin{pmatrix} 1 & \frac{1}{\sqrt{2}}e^{i\phi} \\ \frac{1}{\sqrt{2}}e^{i\phi} & e^{i\psi} \end{pmatrix}. \quad (\text{A2})$$

The unitaries U and W are then defined by the singular value decomposition of Λ :

$$\Lambda = UDW^T, \quad (\text{A3})$$

where $D = \begin{pmatrix} d_H & 0 \\ 0 & d_V \end{pmatrix}$ is the diagonal matrix with eigenvalues equal to the positive square roots of the eigenvalues of $\Lambda^\dagger\Lambda$. In the previous equation, W^T means the transpose in the basis $\{|H\rangle, |V\rangle\}$.

From (A2) it follows that

$$\begin{aligned} |\xi_{\phi,\psi}\rangle &= (UDW^T \otimes 1)(|HH\rangle + |VV\rangle) \\ &= (UD \otimes W)(|HH\rangle + |VV\rangle) \\ &= (U \otimes W)(d_H|HH\rangle + d_V|VV\rangle). \end{aligned} \quad (\text{A4})$$

Let us now find the matrices U and W in an explicit way. By virtue of decomposition (A3), the unitary transformation W^T is the matrix that diagonalizes $\Lambda^\dagger\Lambda$:

$$\Lambda^\dagger\Lambda = (W^T)^\dagger X W^T, \quad (\text{A5})$$

where

$$X = \begin{pmatrix} |x_+|^2 & 0 \\ 0 & |x_-|^2 \end{pmatrix} \Rightarrow D = \begin{pmatrix} |x_+| & 0 \\ 0 & |x_-| \end{pmatrix}, \quad (\text{A6})$$

and x_\pm are defined in (3). The explicit values of the elements of D are

$$d_H = |x_+| = \sqrt{\frac{1}{2} + \frac{\sqrt{2}}{3} \cos\left(\phi - \frac{\psi}{2}\right)},$$

$$d_V = |x_-| = \sqrt{\frac{1}{2} - \frac{\sqrt{2}}{3} \cos\left(\phi - \frac{\psi}{2}\right)}. \quad (\text{A7})$$

From (A5), we find the unitary W as

$$W = \frac{1}{\sqrt{2}} \begin{pmatrix} 1 & 1 \\ e^{i\psi/2} & -e^{i\psi/2} \end{pmatrix}. \quad (\text{A8})$$

Note that the matrices U and W are defined up to the following transformation

$$\begin{aligned} U &\rightarrow UZ, \\ W &\rightarrow WZ^\dagger, \end{aligned} \quad \text{where } Z = \begin{pmatrix} e^{iz_1} & 0 \\ 0 & e^{iz_2} \end{pmatrix}, \quad (\text{A9})$$

and $e^{iz_{1,2}}$ correspond to the global phases chosen for the eigenvectors of $\Lambda^\dagger\Lambda$. Equation (A8) is then only one of the infinite solutions for W .

The matrix U is easily found from (A3):

$$U = \Lambda(W^T)^\dagger D^{-1} = \frac{x_+}{|x_+|} W \begin{pmatrix} 1 & 0 \\ 0 & e^{i\Gamma} \end{pmatrix}, \quad (\text{A10})$$

and Γ is defined in (7):

$$\begin{aligned} \Gamma &= \arg\left(\frac{x_-}{x_+}\right) = \beta - \gamma, \\ \beta &= \arg(\sqrt{2} - e^{i(\phi - \psi/2)}), \\ \gamma &= \arg(\sqrt{2} + e^{i(\phi - \psi/2)}). \end{aligned} \quad (\text{A11})$$

We note that the previous expression of U differs from Eq. (7) for the phase $x_+/|x_+|$. However, this is only a global phase and can be discarded.

Let us now find a more explicit expression for Γ . From the previous equation, we have

$$\begin{aligned} \sin \gamma &= \frac{\sin(\phi - \psi/2)}{\sqrt{3 + \sqrt{8} \cos(\phi - \psi/2)}}, \\ \cos \gamma &= \frac{\sqrt{2} + \cos(\phi - \psi/2)}{\sqrt{3 + \sqrt{8} \cos(\phi - \psi/2)}} \end{aligned} \quad (\text{A12})$$

and

$$\begin{aligned} \sin \beta &= -\frac{\sin(\phi - \psi/2)}{\sqrt{3 - \sqrt{8} \cos(\phi - \psi/2)}}, \\ \cos \beta &= \frac{\sqrt{2} - \cos(\phi - \psi/2)}{\sqrt{3 - \sqrt{8} \cos(\phi - \psi/2)}}. \end{aligned} \quad (\text{A13})$$

The required expression for Γ is then

$$\begin{aligned} \sin \Gamma &= -\frac{2\sqrt{2} \sin(\phi - \psi/2)}{\sqrt{9 - 8 \cos^2(\phi - \psi/2)}}, \\ \cos \Gamma &= \frac{1}{\sqrt{9 - 8 \cos^2(\phi - \psi/2)}}. \end{aligned} \quad (\text{A14})$$

- [1] H. Bechmann-Pasquinucci and A. Peres, *Phys. Rev. Lett.* **85**, 3313 (2000).
- [2] D. Bruß and C. Macchiavello, *Phys. Rev. Lett.* **88**, 127901 (2002).
- [3] N. J. Cerf, M. Bourennane, A. Karlsson, and N. Gisin, *Phys. Rev. Lett.* **88**, 127902 (2002).
- [4] T. Durt, N. J. Cerf, N. Gisin, and M. Żukowski, *Phys. Rev. A* **67**, 012311 (2003).
- [5] N. K. Langford, R. B. Dalton, M. D. Harvey, J. L. O'Brien, G. J. Pryde, A. Gilchrist, S. D. Bartlett, and A. G. White, *Phys. Rev. Lett.* **93**, 053601 (2004).
- [6] G. Molina-Terriza, A. Vaziri, R. Ursin, and A. Zeilinger, *Phys. Rev. Lett.* **94**, 040501 (2005).
- [7] R. T. Thew, A. Acín, H. Zbinden, and N. Gisin, *Phys. Rev. Lett.* **93**, 010503 (2004).
- [8] D. Collins, N. Gisin, N. Linden, S. Massar, and S. Popescu, *Phys. Rev. Lett.* **88**, 040404 (2002).
- [9] D. Kaszlikowski, L. C. Kwek, J.-L. Chen, M. Żukowski, and C. H. Oh, *Phys. Rev. A* **65**, 032118 (2002).
- [10] J. T. Barreiro, N. K. Langford, N. A. Peters, and P. G. Kwiat, *Phys. Rev. Lett.* **95**, 260501 (2005).
- [11] G. Molina-Terriza, A. Vaziri, J. Řeháček, Z. Hradil, and A. Zeilinger, *Phys. Rev. Lett.* **92**, 167903 (2004).
- [12] S. Gröblacher, T. Jennewein, A. Vaziri, G. Weihs, and A. Zeilinger, *New J. Phys.* **8**, 75 (2006).
- [13] M. N. O'Sullivan-Hale, I. A. Khan, R. W. Boyd, and J. C. Howell, *Phys. Rev. Lett.* **94**, 220501 (2005).
- [14] L. Neves, G. Lima, J. G. Aguirre Gomez, C. H. Monken, C. Saavedra, and S. Padua, *Phys. Rev. Lett.* **94**, 100501 (2005).
- [15] Y. I. Bogdanov, M. V. Chekhova, S. P. Kulik, G. A. Maslennikov, A. A. Zhukov, C. H. Oh, and M. K. Tey, *Phys. Rev. Lett.* **93**, 230503 (2004).
- [16] J. C. Howell, A. Lamas-Linares, and D. Bouwmeester, *Phys. Rev. Lett.* **88**, 030401 (2002).
- [17] G. M. D'Ariano, P. Mataloni, and M. F. Sacchi, *Phys. Rev. A* **71**, 062337 (2005).
- [18] C. H. Bennett and G. Brassard, in *Proceedings of the IEEE International Conference on Computers, Systems and Signal Processing, Bangalore, India* (IEEE, New York, 1984), p. 175.
- [19] W. K. Wootters, *Found. Phys.* **16**, 391 (1986).
- [20] M. Barbieri, F. De Martini, G. Di Nepi, P. Mataloni, G. M. D'Ariano, and C. Macchiavello, *Phys. Rev. Lett.* **91**, 227901 (2003).
- [21] M. Barbieri, F. De Martini, G. Di Nepi, and P. Mataloni, *Phys. Rev. Lett.* **92**, 177901 (2004).
- [22] C. Cinelli, G. Di Nepi, F. De Martini, M. Barbieri, and P. Mataloni, *Phys. Rev. A* **70**, 022321 (2004).
- [23] M. Barbieri, F. De Martini, G. Di Nepi, and P. Mataloni, *Phys. Lett. A* **334**, 23 (2005).
- [24] D. F. V. James, P. G. Kwiat, W. J. Munro, and A. G. White, *Phys. Rev. A* **64**, 052312 (2001).